Improved electrochemical performance of the LiNi$_{0.8}$Co$_{0.1}$Mn$_{0.1}$O$_2$ material with lithium-ion conductor coating for lithium-ion batteries

CrossMark

Meng Wang[a,*], Ran Zhang[a,c], Yongqiang Gong[a,c], Yuefeng Su[b], Debo Xiang[a], Lin Chen[a], Yunbo Chen[a], Min Luo[a,c], Mo Chu[c]

[a] Advanced Manufacture Technology Center, China Academy of Machinery Science and Technology, Beijing 100083, China
[b] School of Materials Science and Engineering, Beijing Institute of Technology, Beijing 100081, China
[c] College of Chemical and Environmental Engineering, China University of Mining and Technology, Beijing 100083, China

ARTICLE INFO

ABSTRACT

The LiNi$_{0.8}$Co$_{0.1}$Mn$_{0.1}$O$_2$ was coated by a lithium-ion conductor Li$_3$PO$_4$ layer using a simple and efficient coating method. The Ni$_{0.8}$Co$_{0.1}$Mn$_{0.1}$(OH)$_2$ precursor serves as a coating target, and Li$_3$PO$_4$ was deposited on its surface. This method avoids forming lithium residuals and twice calcination process. The electrochemical measurements demonstrated the electrochemical performance of LiNi$_{0.8}$Co$_{0.1}$Mn$_{0.1}$O$_2$ is greatly enhanced by coating with lithium ion conductor Li$_3$PO$_4$, especially at high work potential. It can be ascribed to the Li$_3$PO$_4$ acted as a protection layers to reduce the side reactions between the cathode material and electrolyte, and therefore reduced the surface and charge transfer resistance during cycling. Besides that, the high lithium ion conductor characteristics of Li$_3$PO$_4$ coating layer are beneficial to improve the diffusion coefficient of lithium ions.

1. Introduction

Ni-rich layered cathode material is considered to be one of the most promising alternative material for lithium-ion batteries, due to its high reversible capacity (about 200 mAh g^{-1}), lower cost and environmentally friendly [1–3]. However, the problem of undesirable thermal stability, inferior cycle performance and strict storage conditions hinder the practical application of Ni-rich layered oxide LiNi$_{0.8}$Co$_{0.1}$Mn$_{0.1}$O$_2$ material. At elevated voltage, the unstable Ni^{4+} at the surface of Ni-rich materials can be reduced to Ni^{2+} accompanied by the formation of spinel phase or inactive rock salt phase. These impure phases will hinder the diffusion of lithium ions, cause fast electrode polarization and rapid capacity fading [4–8]. In addition, the active materials react with HF which produced by decomposition of electrolyte to form solid-electrolyte interphase (SEI) and therefore the interfacial impedance of electrode increased during cycling [9]. Besides that, when the materials exposed to air, it has redox reaction between cathode materials and moisture in the atmosphere, result in the reduction of Ni^{3+} to Ni^{2+} accompanied by forming unwanted Li$_2$CO$_3$ and LiOH on particles surface [10–13].

So far, in order to improve the electrochemical properties of layered Ni-rich oxide cathode materials, massive efforts have been devoted to settle above issues. Generally speaking, there are two main modification methods. One way is to improve structure stability via doping with metallic ions, such as Mg^{2+}, Al^{3+}, Cr^{3+} [8,14,15]. Another strategy is to modify surface by coating with phosphate, metal oxides, and fluoride as a barrier to prevent active materials from undermining by electrolyte [16,17]. However, most of the coating materials are lithium ion insulator which could hinder the migration of lithium ions. Unlike above review, lithium-ion conductor Li$_3$PO$_4$ has strong bonding energy of PO$_4$$^{3-}$ can inhibit the side reactions between materials and electrolytes. Furthermore, Li$_3$PO$_4$ is an excellent lithium ion conductor with a high ionic conductivity (10^{-6}–10^{-8} S cm^{-1}) which could promote the diffusion of lithium ions [18,19]. In addition, most of the reported coating processes were carried out directly on the surface of the cathode materials via disperse the cathode materials into water, but the alkalinity of the coated final materials is usually increased owing to the employment of water as a solvent. The dissolved Li species could react with water during the coating process, led to form Li$_2$CO$_3$ and LiOH impurities, which can deteriorate cathode and further affect the performance of the materials [20].

In our work, we employed commercial spherical hydroxide precursor Ni$_{0.8}$Co$_{0.1}$Mn$_{0.1}$(OH)$_2$ as a coating target, and Li$_3$PO$_4$ was deposited on its surface. The advantage of this method is that it avoids the two calcination process and the contact between product and water. The effect of Li$_3$PO$_4$ on the electrochemical properties of LiNi$_{0.8}$Co$_{0.1}$Mn$_{0.1}$O$_2$ was investigated in detail.

* Corresponding author.
  E-mail address: wangm@camtc.com.cn (M. Wang).

Table 1
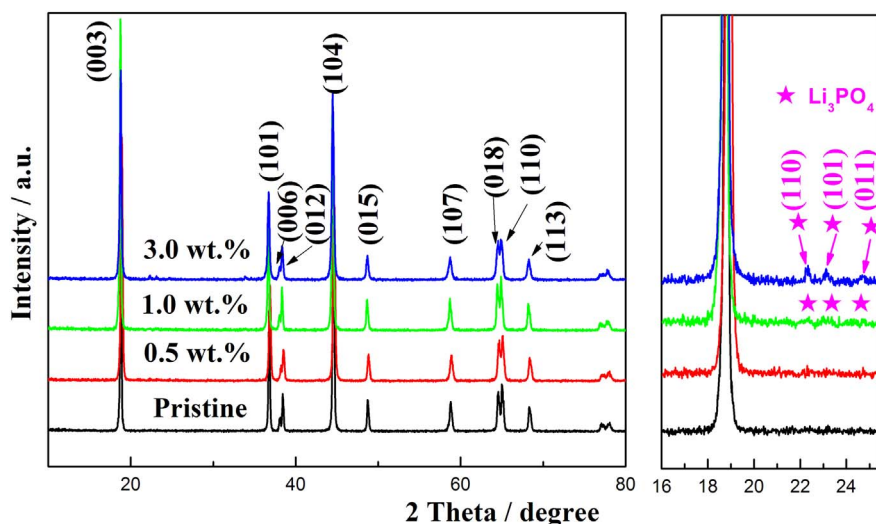Lattice parameters of the pristine and Li_3PO_4-coated NCM811.

Samples	$a(Å)$	$c(Å)$	c/a	$I_{(003)}/I_{(104)}$
Pristine	2.872	14.178	4.937	1.114
0.5 wt%	2.868	14.169	4.940	1.307
1.0 wt%	2.871	14.198	4.945	1.389
3.0 wt%	2.875	14.198	4.938	1.225

2. Experimental

2.1. Samples synthesis

The pristine $LiNi_{0.8}Co_{0.1}Mn_{0.1}O_2$ (NCM811) was prepared by mixing commercial spherical precursor $Ni_{0.8}Co_{0.1}Mn_{0.1}(OH)_2$ and $LiOH·H_2O$ at a molar ration of 1:1.05 (a 5 wt% excess amount of $LiOH·H_2O$ was used to compensate the loss of Li during sintering process at high temperatures). The powder was preheated at 450 °C for 6 h in air, then sintered at 800 °C for 12 h in an O_2 flow. The Li_3PO_4-coated NCM811 was synthesized by the following method. At first, stoichiometric lithium hydroxide monohydrate (a 5.0 wt% excess) and 15 g $Ni_{0.8}Co_{0.1}Mn_{0.1}(OH)_2$ was slowly poured into a continuously stirring reactor with 100 ml deionized water. Then $(NH_4)_2HPO_4$ dissolved into 50 ml deionized water and fed into the above mentioned solution. The homogenous suspension was stirred and evaporated at 85 °C Then the obtained mixture was preheated at 450 °C for 6 h in air, and sintered at 800 °C for 12 h in an O_2 flow. The coating content of Li_3PO_4 is 0.5 wt%, 1.0 wt% and 3.0 wt% to the NCM811. The ideal chemical reaction can be expressed by the formula (1):

$$(NH_4)_2HPO_4 + 3LiOH \rightarrow 2NH_3 \uparrow + 3H_2O + Li_3PO_4 \tag{1}$$

2.2. Materials characterization

Powder X-ray diffraction (XRD, UltimaIV-185) measurements was employed to identify the crystal structures of the prepared samples equipped with a Cu Kα radiation in the 2θ range of 10–90° at a scan rate of 8° min^{-1}. The observation of samples surface morphology was carried out using Field emission scanning electron microscopy (FESEM, XL 30S-FEG, FEI Co., 10 kV). High resolution transmission electron microscopy (HRTEM) was applied to observe the coating layer and microstructure of the materials on a JEOL-JEM-2100F.

2.3. Electrochemical measurements

The electrochemical performance of the pristine and Li_3PO_4-coated NCM811 were evaluated by CR2025-type coin cells with metallic lithium as the counter electrode, and Celgard 2300 membrance as a separator. The positive electrode were fabricated by 85 wt% active cathode material, 10 wt% acetylene black and 5 wt% polyvinylidence fluoride (PVDF) binder dissolved in *N*-methyl-2-pyrrolidone to form a homogeneous slurry. The viscous slurry was coated on an aluminum foil current collector and dried in a vacuum oven at 60 °C for 12 h to remove the solvent. The obtained film were pressed and punched to the round disks with a diameter of 12 mm. The cells were assembled in an argon-filled glove box with an electrolyte of 1 M $LiPF_6$ dissolved in a mixture of ethylene carbonate (EC)-dimethyl carbonate (DMC)-ethyl methyl carbonate (EMC) (1:1:1 in volume). Galvanostatic charge/discharge experiments were conducted on a multi channel battery test system of CT2001A land (Wuhan, China) between different voltage rang of 2.8–4.3 V and 2.8–4.5 V (versus Li/Li^+). The charge/discharge current density was 0.1C/1.0C of the cycling performance tests (1.0C = 150 mA g^{-1}). The electrochemical impedance spectra (EIS) was measured at a CHI 604D electrochemical workstation in the frequency range of 0.01 HZ to 100 KHZ, the amplitude of potentisatatic signal was 5 mV. To observe the changes of the cathode materials, the cells were disassembled after 50 cycles and the cathode electrodes were washed by DMC in a glove box.

3. Results and discussion

3.1. X-ray diffraction and morphology

Fig. 1 shows the X-ray diffraction patterns of the pristine and Li_3PO_4-coated NCM811. It can be observed that all the main diffraction peaks are sharp, which indicates that the samples keep excellent crystallinity that can be indexed to a hexagonal α-NaFeO$_2$ layered structure with a space group of $R\bar{3}m$. In the structure, Li atoms occupy in 3a sites, the transition metal (Ni, Mn, Co) atoms occupy the 3b sites and O in 6c sites. The distinct splitting of (006)/(012) and (018)/(110) peaks are consistent with a well order layered structure for all samples [21]. The enlarged XRD patterns in the range of 16–26° are shown in the right of Fig. 1. The peaks relating to Li_3PO_4 can be observed for the Li_3PO_4-coated samples, which are (110), (101) and (011) peaks [22]. These peaks become obviously with the coating content of Li_3PO_4 increased to 3.0 wt%. Table 1 shows the lattice parameters of pristine and Li_3PO_4-coated MCN811 calculated from the X-ray diffraction patterns using MDIJADE6. The intensity ration of $I_{(003)}/I_{(104)}$ depends on the degree of
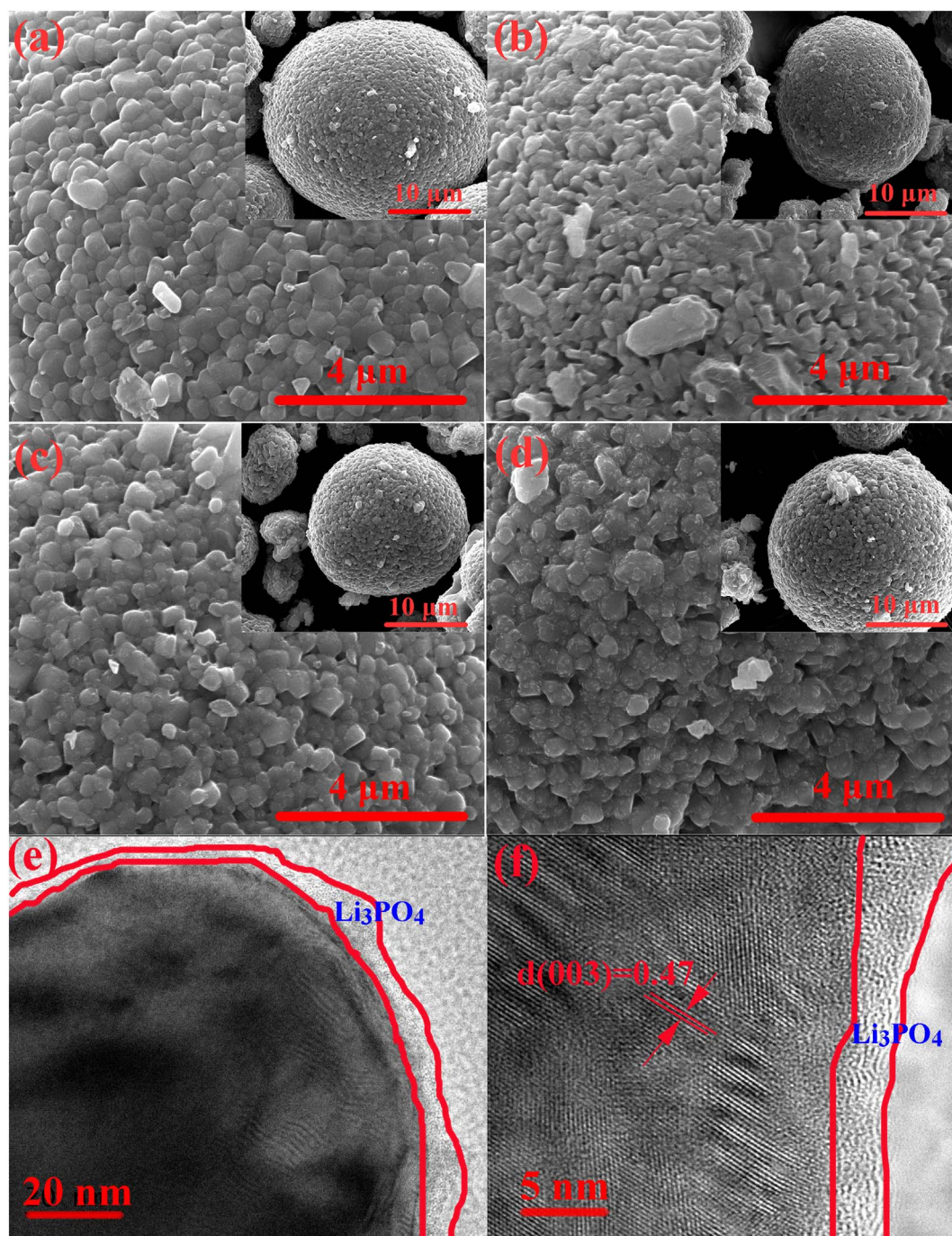
Fig. 2. FESEM images of the (a) pristine, (b) 0.5 wt%, (c) 1.0 wt% and (d) 3.0 wt% Li₃PO₄-coated NCM811; (e) and (f) HRTEM images of 3.0 wt% Li₃PO₄-coated NCM811.

displacement between ions located at the 3a and 3b sites, and it < 1.2 is an indicator of the cation mixing [23]. Such unwanted cation mixing is supposed to deteriorate the layered structure and leads to undesirable electrochemical performance [24]. It can be obtained from Table 1 that the $I_{(003)}/I_{(104)}$ value of pristine NCM811 is < 1.2, which means the cations mixing phenomenon of it is serious. The lattice parameter a indicates the metal-metal interlayer distance while c represents the average metal–metal interslab distance [25,26]. The large c is generally associated with fast Li-ion insertion/extraction [27,28]. The 1.0 wt% Li₃PO₄-coated sample shows the highest c, implying that it have the largest channels for lithium ions intercalation and deintercalation transportation process [26]. High c/a value indicates that the lattice has the priority to grow along the c axis, and it also indicates small cation mixing degree and a well-defined hexagonal layered structure [29,30].

The 1.0 wt% Li₃PO₄-coated samples shows the highest c/a value, implying the best ordered layered hexagonal structure in it.

Fig. 2 presents the surface morphology images of as-prepared samples by field emission scanning electron microscopy (FESEM) and high resolution transmission electron microscopy (HRTEM). It can be seen that all the samples are micro-sized spherical secondary particles with average diameters of about 20–25 μm, which are made up of nanosized primary particles with a size of about 300–400 nm. The surface of pristine NCM811 is clean and smooth. With the increase of coating quality, the surface of Li₃PO₄-coated materials becoming more and more rough. When the content of Li₃PO₄ reached to 3.0 wt%, the sphere surface is covered by many small particles. As can be seen from the Fig. 2(e) and (f), a coating layer of about 4–8 nm is clearly seen on the surface of the 3.0 wt% Li₃PO₄-coated NCM811. The thick and dense
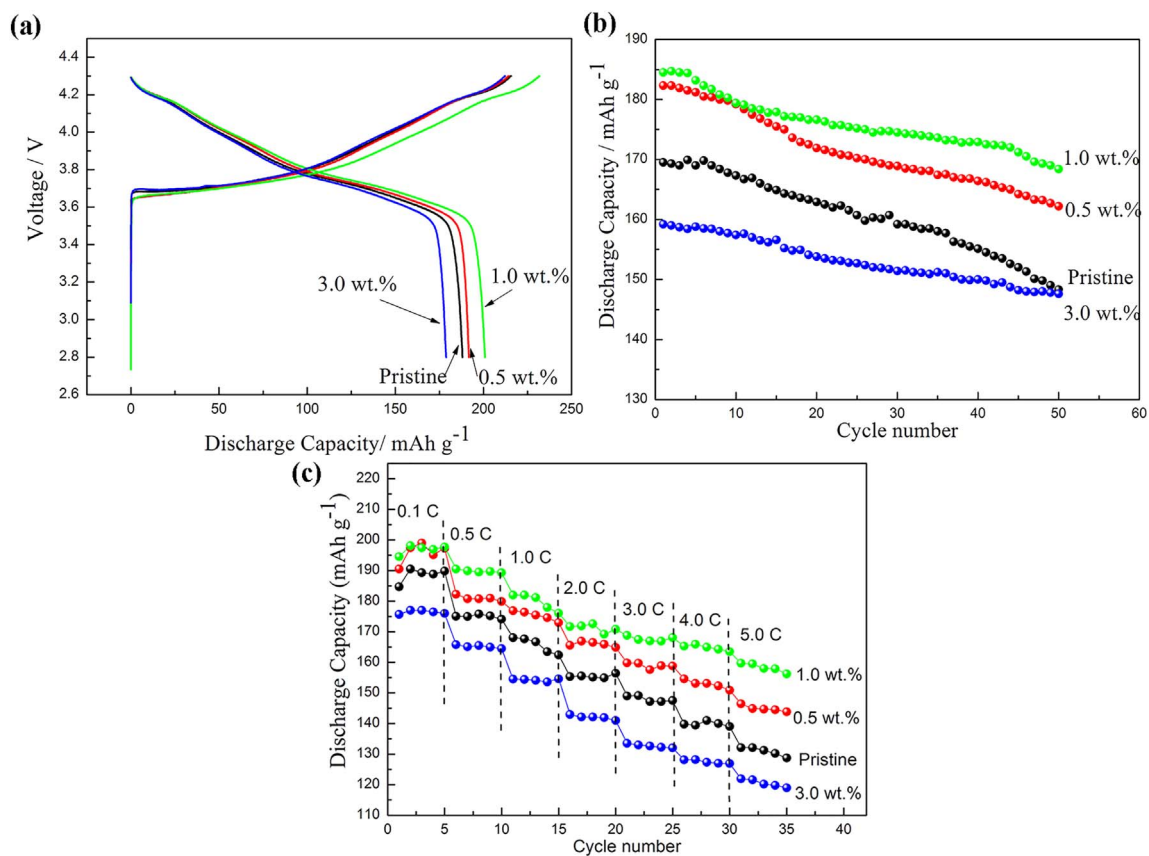
Fig. 3. (a) The initial charge-discharge profiles, (b) cycling performance curves and (c) rate performance of the pristine and Li$_3$PO$_4$-coated NCM811 in the range of 2.8–4.3 V.
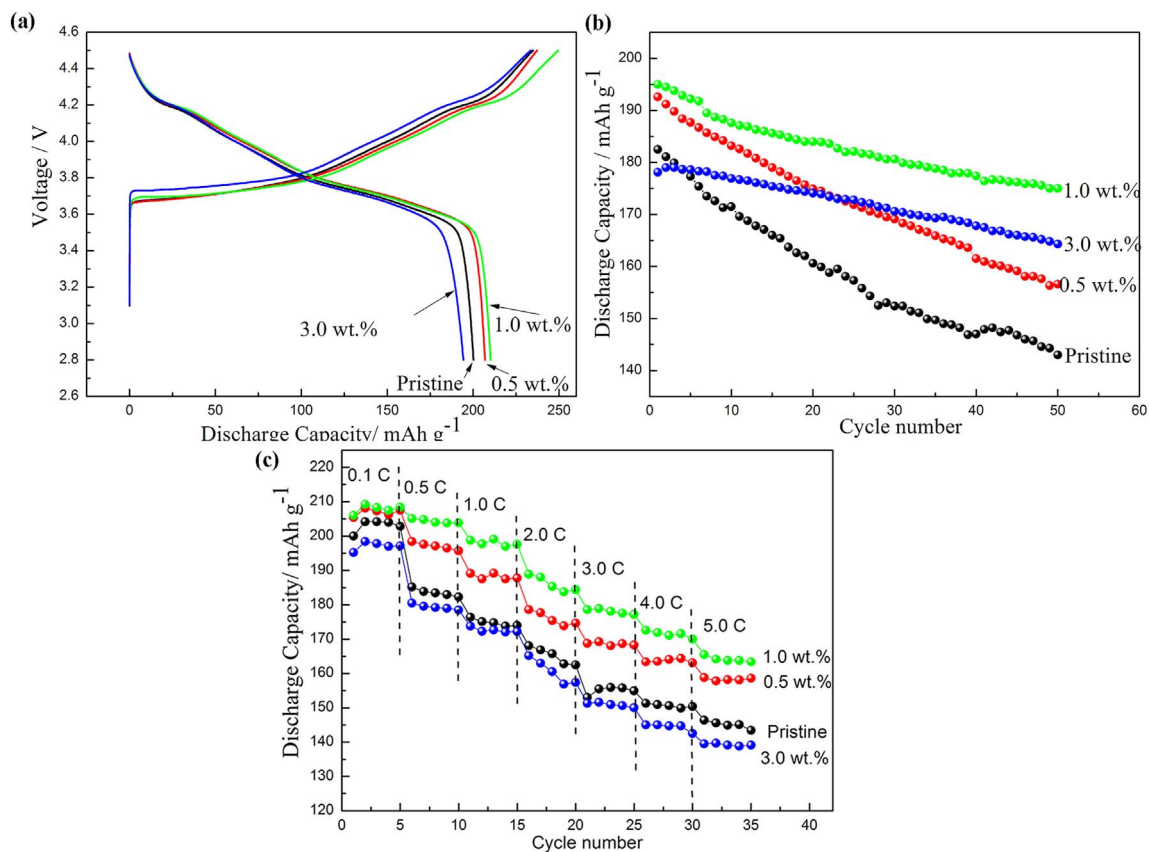

Fig. 4. The (a) initial charge-discharge profiles, (b) cycling performance curves, (c) rate performance of the pristine and Li$_3$PO$_4$-coated NCM811 in the range of 2.8–4.5 V.
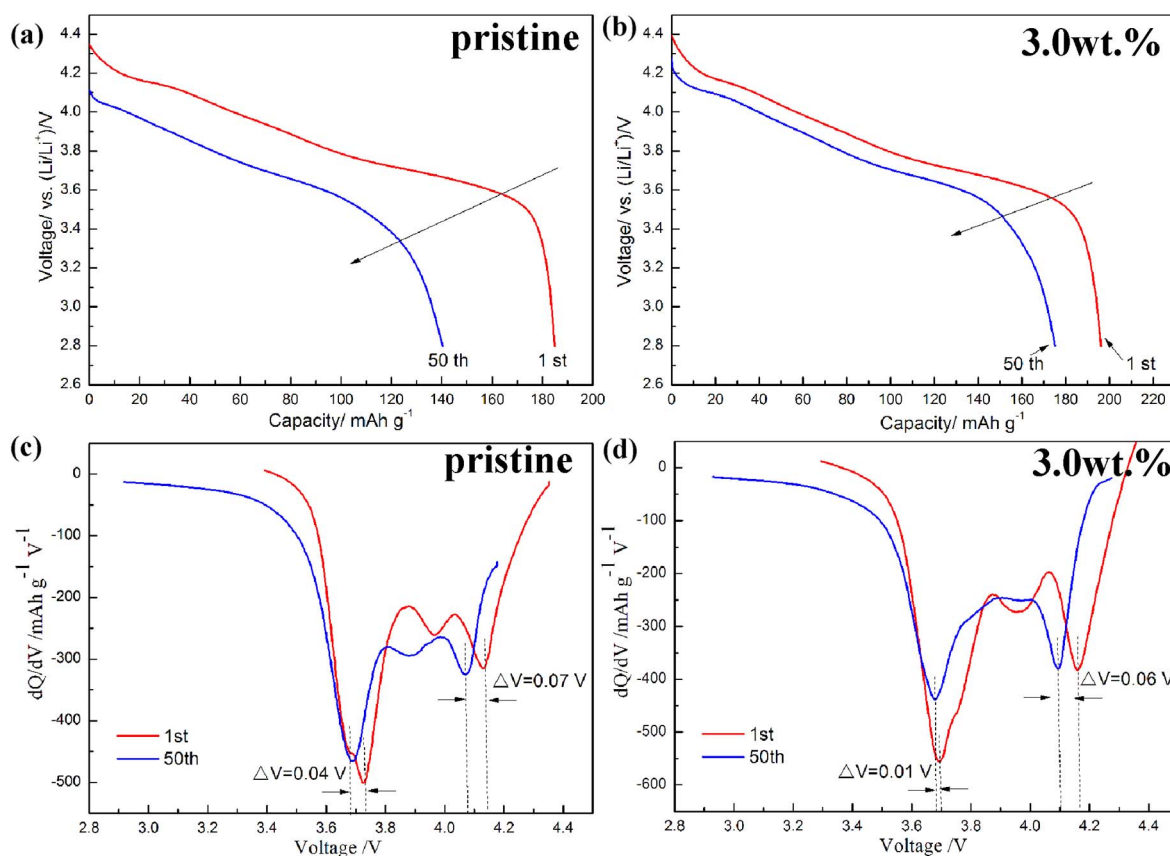
Fig. 5. The discharge curves (a, b) and dQ/dV plots of discharge curves (c, d) for pristine NCM811 and 3.0 wt% Li_3PO_4-coated NCM811.
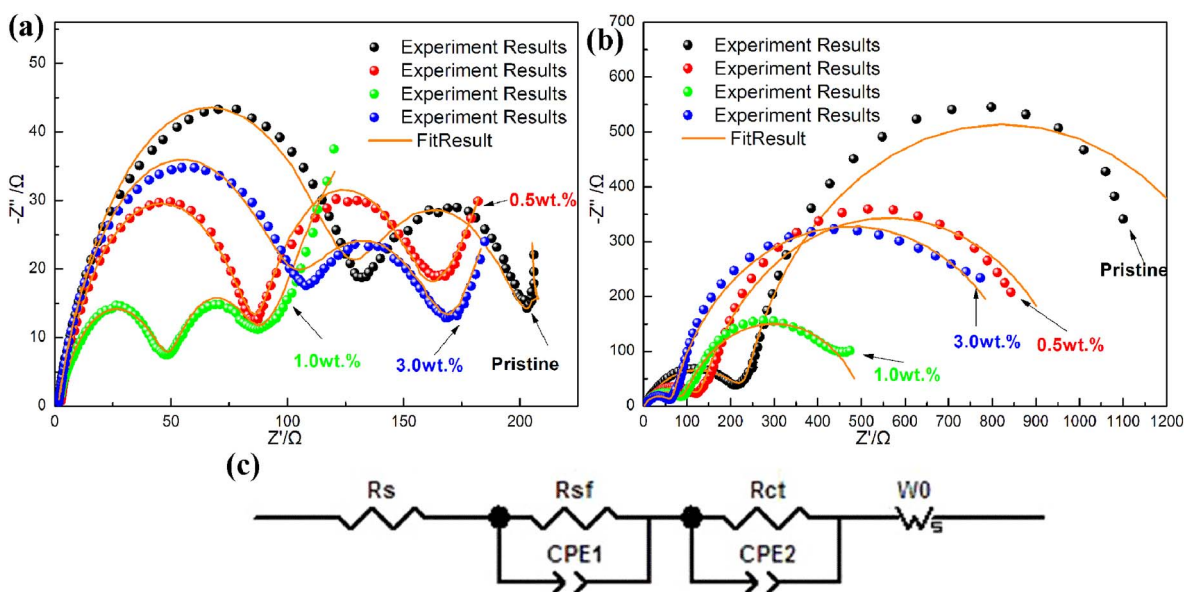

Fig. 6. The Nyquist plots of the cells with the pristine and Li_3PO_4-coated NCM811 after the 1st cycle (a), 50th cycle (b) and the equivalent electrical circuit (c).

Li_3PO_4 coating layer of the material can efficiently protect the active materials against HF attack in electrolyte, which largely enhance the cycling performance of cells. The Fig. 2(f) illustrates the sample has the *d* spacing of (003) plane is 0.47 nm which is the same as that reported in other literature [31]. The result indicates that coating processes modify the surface of cathode material without changing its bulk crystalline structure.

3.2. Electrochemical performances

Fig. 3 compares the electrochemical properties of the pristine nd Li_3PO_4-modified NCM811 in the range of 2.8–4.3 V. The initial charge-discharge curves at 0.1C are shown in Fig. 3a. The discharge specific capacity of pristine NCM811 delivers 188.1 mAh g^{-1}, while the 0.5 wt % and 1.0 wt% Li_3PO_4-coated NCM811 present a higher discharge capacity than the pristine NCM811, which are 191.7 mAh g^{-1} and 200.8 mAh g^{-1}, respectively. The improved discharge capacity for the

Table 2
Fitting values of the electrochemical impedance profiles of the pristine and Li$_3$PO$_4$-modified NCM811.

Sample	At the 1st cycle			At the 50th cycle		
	R$_s$ (Ω)	R$_{sf}$ (Ω)	R$_{ct}$ (Ω)	R$_s$ (Ω)	R$_{sf}$ (Ω)	R$_{ct}$ (Ω)
Pristine	1.4	125.9	76.45	2.0	237.5	1172
0.5 wt%	1.5	100.5	64.4	1.0	134.7	854.8
1.0 wt%	1.4	48.6	31.4	1.5	91.2	415.1
3.0 wt%	2.4	84.6	65.1	1.8	64.9	821.3

0.5 wt% and 1.0 wt% Li$_3$PO$_4$-coated NCM811 can be due to the Li$_3$PO$_4$ facilitates the migration of lithium ions and suppression of the reaction between the cathode surface and the electrolyte which will improve the utilization efficiency of lithium ions [32,33]. However, the 3.0 wt% Li$_3$PO$_4$-coated NCM811 displays the lowest discharge capacity of 178.8 mAh g^{-1}, which is attributed to its high amount of non-electrochemical active material Li$_3$PO$_4$. Fig. 3b illustrates the cycling performance of the as-prepared materials at 1.0C. As can been seen, the capacities retention of the 0.5 wt%, 1.0 wt% and 3.0 wt% Li$_3$PO$_4$-coated NCM811 after 50 cycles are 89.0%, 91.3%, 94.1%, respectively, which are higher than that of the pristine NCM811 (87.6%). It reveals that Li$_3$PO$_4$ coating layer can isolate the cathode materials from direct contacting with the electrolyte, resulting in the enhanced structure stability and cycling performances [34]. With the increase of coating amount, the cycle performance gradually enhanced which can be due to the decreased contact area between electrodes and electrolyte. Fig. 3c demonstrates the rate performance of the pristine and Li$_3$PO$_4$-modified NCM811, the cells were charged at 0.1C and discharged at various current rates. According to the previous report [35], the capacity fade is accelerated when discharged at high rates. The discharge capacities and the capacity retention rate of the 1.0 wt% Li$_3$PO$_4$-coated NCM811 at varied discharge current rates are highest. For example, the capacity discharge capacity at 5.0C is 159.7 mAh g^{-1}, with the capacity retention of 82.9% when compared to the discharge capacity at 0.1C. In the contrast, the capacity retention of the pristine material at 5.0C is only 71.5%. However, the 3.0 wt% Li$_3$PO$_4$-coated NCM811 has the worst rate performance, the discharge capacity only remains 121.9 mAh g^{-1} at 5.0C, with the capacity retention of 69.4% when compared to the discharge capacity at 0.1C. It indicates that too thick coating layer cannot effectively improve the rate performance of the materials.

The high cutoff voltage (> 4.3 V) may deteriorate Ni-rich materials and form spinel phase or inactive rock salt phase. Therefore, the electrochemical properties of the materials between 2.8 and 4.5 V are tested and the results are shown in the Fig. 4. The initial charge-discharge curves at 0.1C are shown in Fig. 4a. The initial reversible discharge

capacities are 200.2, 206.8, 207.0 and 194.3 mAh g^{-1} for the pristine, 0.5, 1.0 and 3.0 wt% Li$_3$PO$_4$-coated NCM811, respectively. The 1.0 wt% Li$_3$PO$_4$-coated NCM811 still has the highest discharge capacity. The discharge capacity are higher than that obtained at the cutoff voltage of 4.3 V, which are benefit from the high charge voltage makes more lithium ions extract from the lattice. However, the cathode irreversible phase transformation occurs easily at high cutoff voltage, leading to fast capacity decay when compared with that in the range of 2.8–4.3 V. The cycling performance at 1.0C are shown in Fig. 4b. Obviously, the capacity retention of the coated materials are significantly improved, which are 81.3, 88.7 and 93.2% for the 0.5, 1.0 and 3.0 wt% Li$_3$PO$_4$-coated NCM811, respectively, while that of the pristine NCM811 is only 78.4%. The undesirable cycling performance of Ni-rich materials is attributed to the unstable Ni^{4+} ions in the high delithiated materials which could cause the destruction of layered structure [33]. After coating, the Li$_3$PO$_4$ layer isolates the cathode material from electrolyte, which suppress the production of oxygen and corrosion of the HF form electrolyte. Although the capacity retention of 3.0 wt% Li$_3$PO$_4$-coated sample is highest of all (93.2%), the 1.0 wt% Li$_3$PO$_4$-coated material possesses the highest discharge capacities of 175.9 mAh g^{-1} after cycling with the capacity retention of 88.7%. That means excessive Li$_3$PO$_4$ coating layer can improve the cycling performance of the material, but not conductive to the enhancement of the discharge capacity. Fig. 4c presents the rate properties of the samples. It is clearly that the 1.0 wt% Li$_3$PO$_4$-coated NCM811 deliver the highest discharge capacity at all current rates. The discharge capacity remains of the 1.0 wt% Li$_3$PO$_4$-coated material is 165.5 mAh g^{-1} at 5.0C, with the capacity retention of 80.3% when compared to the discharge capacity at 0.1C, and while the capacity retention of the pristine at 5.0C only remains 73.2%. When the Li$_3$PO$_4$ amount increased to 3.0 wt%, the capacity retention at 5.0C is decreased to 71.0% when compared to the discharge capacity at 0.1C. That reveals proper Li$_3$PO$_4$ coating amount can promote lithium ion migration, which due to its ionic conducting property [36]. However, too thick coating layer is detrimental to the electrochemical properties of the materials, although it is a lithium ion conductor.

The discharge curves (2.8–4.5 V) of the 1st and the 50th at 1.0C for the pristine and 3.0 wt% Li$_3$PO$_4$-coated NCM811 are shown in Fig. 5(a, b). Obviously, the voltage of pristine NCM811 electrode after cycling shows a sharply drop, while that of the 3.0 wt% Li$_3$PO$_4$-coated NCM811 shows a minimum drop. Fig. 5c and d presents the dQ/dV plots of discharge curves for pristine NCM811 and 3.0 wt% Li$_3$PO$_4$-coated NCM811 at the 1st and 50th. In contrast to the pristine one, Li$_3$PO$_4$-coated NCM811 shows much less voltage fade during the long-term cycling test. One of the major reasons for the voltage decay of the NCM cathode materials upon cycling is that contaminating species are usually found on the electrode surface, and these surface residual species can react with the electrolyte forming insulating layer [37–39].
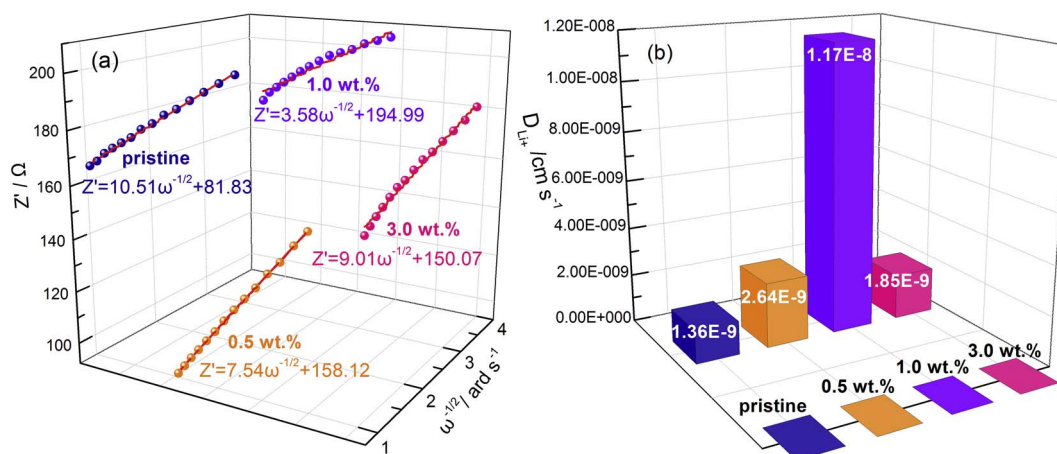

Fig. 7. (a) the profiles of Z' vs. $\omega^{-1/2}$; (b) D_{Li^+} obtained from the EIS data.

And the unstable dilithium structure which can induce the active Ni ions migrating to the adjacent Li ions sites. This ions migration gives rise to serious phase variation from layered to spinel-like or rock salt structures, hence accelerates the electrode capacity fading [40–43]. In addition, the parasitic side reactions between pristine NMC and electrolyte cause sever transition metal ions dissolution, thus resulting in the collapse of the surface lattice structure. Therefore, the main mechanism of improvement after coating can be assigned to minimizing harmful side reactions by forming a protective layer at the interface between active material and electrolyte. The remarkable cycling stability of the Li_3PO_4-coated NCM811 indicates that the coating layer is facile for Li ion diffusion and effectively alleviates decomposition of electrolyte and reduce electrochemical polarization on the surface of NCM811 particles.

To investigate the reasons for the notably improved electrochemical performance of the Li_3PO_4-coated NCM811, the electrochemical impedance spectroscopy (EIS) measurements are carried out for the pristine and Li_3PO_4-coated NCM811 after the 1st and 50th cycles at 1.0C (between 2.8 V and 4.5 V) and then charged to 4.3 V. And the results are shown in Fig. 6. The Nyquist plots of the pristine and Li_3PO_4-coated NCM811 consist of a semicircle in high-frequency region is attributed to the resistance of Li^+ diffusion though the surface film (R_{sf}), a semicircle in middle-frequency region is assigned to the charge transfer resistance (R_{ct}) and a sloped straight line in low-frequency region is ascribed to Li^+ diffusion process in the bulk (Z_w) [44]. The experimental data are simulated by ZView software, which are obtained according to the equivalent circuit and the values are listed in Table 2. We can find that there are no significant difference of the electrolyte impedance (R_s) between the pristine and Li_3PO_4-coated NCM811. However, the R_{sf} and R_{ct} values of Li_3PO_4-coated NCM811 are much smaller than that of the pristine NCM811. The Li_3PO_4 coating layer can suppress the rising of the solid electrolyte interface film impedance and the charge transfer resistance obviously. Especially, the R_{sf} and R_{ct} of the pristine sample are 125.9 Ω and 76.5 Ω at the 1st cycle, and drastically increases to 237.5 Ω and 1172.0 Ω after 50 cycles, respectively. In contrast, the R_{sf} and R_{ct} values of 1.0 wt% Li_3PO_4-coated NCM811 are only 48.6 Ω and 31.4 Ω at the 1st cycle, and slowly increases to 91.2 Ω and 415.1 Ω after 50 cycles, respectively. And after 50 cycles, the increase of $R_{sf} + R_{ct}$ values for 1.0 wt% Li_3PO_4-coated NCM811 are greatly depressed. The present of Li_3PO_4 coating layer can effectively suppress the increase of SEI layer and charge transfer resistance, which will facilitate the diffusion of Li^+ ions. As a consequence, the electrochemical performance of Li_3PO_4-coated NCM811 are improved, which is good agreement with above descriptions.

As mentioned above, the straight sloping line at low frequency region is attributed to the lithium ions diffusion in the bulk of the materials (in Fig. 6a). Therefore, the diffusion coefficient of lithium ions (D_{Li^+}) can be calculated from the slop in the low frequency region according to the following equation [45,46]:

$$D_{Li^+} = \frac{R^2 T^2}{2n^4 F^4 A^2 C_{Li^+}^2 \sigma^2} \qquad (2)$$

C_{Li^+} is the concentration of lithium ions in the materials, R is the gas constant, T is the absolute temperature, F is the Faraday constant, A refers to the electrochemically active surface area (here is surface area of the electrode), n stands for the number of electrons per molecule during redox process, σ is the Warburg factor which can be obtained by the following equation:

$$Z' = R_s + R_{ct} + \sigma \omega^{1/2} \qquad (3)$$

Z' is the real part of impedance, R_s is the electrolyte resistance, R_{ct} is the charge transfer resistance and ω is the angular frequency. Fig. 7(a) shows the linear relationship of Z' and $\omega^{-1/2}$ and the slope of the fitted straight line indicates the σ value. According to the Eqs. (2) and (3), D_{Li^+} values are calculated and compared in Fig. 7(b). It is clearly that the

diffusion coefficient of lithium ions are increased after coating, and that of the 1.0 wt% Li_3PO_4-coated NCM811 reaches 1.17×10^{-8} cm s^{-1}, which is one order higher than that of the pristine sample. This proves that the Li_3PO_4 coating can effectively promote the migration rate of lithium ions.

4. Conclusions

In this work, the commercial $Ni_{0.8}Co_{0.1}Mn_{0.1}(OH)_2$ precursor was employed as coating target, and Li_3PO_4 was deposited on its surface. This process can avoid the contact of active materials with water and twice sintering process. The results show the Li_3PO_4-modified NCM811 present excellent electrochemical performance. The 1.0 wt% Li_3PO_4-modified NCM811 has the highest discharge capacity and best rate performance. The 3.0 wt% Li_3PO_4-modified NCM811 processes the most excellent cycling performance but the discharge capacity and rate performance are damaged due to the excessive coating amount. The increase of $R_{sf} + R_{ct}$ values for Li_3PO_4-coated NCM811 are greatly depressed after 50 cycles. It proved that an appropriate amount and uniformly Li_3PO_4 coating layer can block active materials from direct contact with electrolyte and effectively suppress side reactions between cathode surface and electrolyte. The high ionic conductivity of Li_3PO_4 coating layer are benefit for improving the diffusion rate of Li^+ ions, the D_{Li^+} of 1.0 wt% Li_3PO_4-coated NCM811 reaches 1.17×10^{-8} cm s^{-1}, which is one order higher than that of the pristine sample. Therefore, surface modification by Li_3PO_4 is an effective method to enhance the properties of $LiNi_{0.8}Co_{0.1}Mn_{0.1}O_2$ cathode materials and is expected to solve cycling problems for the applications of Ni-rich cathode materials in high specific capacity lithium ion batteries.

References

[1] G.V. Zhuang, G. Chen, J. Shim, X. Song, P.N. Ross, T.J. Richardson, Li_2CO_3 in $LiNi_{0.8}Co_{0.15}Al_{0.05}O_2$ cathodes and its effects on capacity and power, J. Power Sources 134 (2004) 293–297.
[2] K. Shizuka, C. Kiyohara, K. Shima, Y. Takeda, Effect of CO_2 on layered $Li_{1+z}Ni_{1-x-y}Co_xM_yO_2$ (M=Al, Mn) cathode materials for lithium ion batteries, J. Power Sources 166 (2007) 233–238.
[3] H.S. Liu, Y. Yang, J.J. Zhang, Investigation and improvement on the storage property of $LiNi_{0.8}Co_{0.2}O_2$ as a cathode material for lithium-ion batteries, J. Power Sources 162 (2006) 644–650.
[4] S.H. Wang, W. Chang, S.M. Kim, D. Su, D.H. Kim, J.Y. Lee, K.Y. Chung, E.A. Stach, Investigation of changes in the surface structure of $Li_xNi_{0.8}Co_{0.15}Al_{0.05}O_2$ cathode materials induced by the initial charge, Chem. Mater. 26 (2014) 1084–1092.
[5] F. Lin, I.M. Markus, D. Nordlund, T.C. Weng, M.D. Asta, H.L. Xin, M.M. Doeff, Surface reconstruction and chemical evolution of stoichiometric layered cathode materials for lithium-ion batteries, Nat. Commun. 5 (2014) 3529–3537.
[6] S.K. Jung, H. Gwon, J. Hong, K.Y. Park, D.H. Seo, H. Kim, J. Hyun, W. Yang, K. Kang, Understanding the degradation mechanisms of $LiNi_{0.5}Co_{0.2}Mn_{0.3}O_2$ cathode materials in lithium ion batteries, Adv. Energy Mater. 4 (2014) 94–98.
[7] L. Wu, K.W. Nam, X.J. Wang, Y.N. Zhou, J.C. Zheng, X.Q. Yang, Y.M. Zhu, Structural origin of overcharge-induced thermal instability of Ni-containing layered cathode for high-energy-density lithium batteries, Chem. Mater. 23 (2011) 3953–3960.
[8] X.H. Xiong, Z.X. Wang, H.J. Guo, Q. Zhang, X.H. Li, Enhanced electrochemical properties of lithium-reactive V_2O_5 coated on the $LiNi_{0.8}Co_{0.1}Mn_{0.1}O_2$ cathode material for lithium ion batteries at 60 ℃, J. Mater. Chem. A 1 (2013) 1284–1288.
[9] S.J. Yoon, K.J. Park, B.B. Lim, C.S. Yoon, Y.K. Sun, Low temperature electrochemical properties of $Li[Ni_xCo_yMn_{1-x-y}]O_2$ cathode materials for lithium batteries, J. Electrochem. Soc. 162 (2015) A3059–A3063.
[10] G.V. Zhuang, G. Chen, J. Shim, X. Song, P.N. Ross, Li_2CO_3 in $LiNi_{0.8}Co_{0.15}Al_{0.05}O_2$, J. Power Sources 134 (2004) 293–297.
[11] S.W. Song, G.V. Zhuang, P.N. Ross, A study of surface film formation on $LiNi_{0.8}Co_{0.15}Al_{0.05}O_2$ cathodes using attenuated total reflection infrared spectroscopy, J. Electrochem. Soc. 151 (2004) A1162–A1167.
[12] K. Shizuka, C. Kiyohara, K. Shima, Y. Takeda, Effect of CO_2 on layered $Li_{1+z}Ni_{1-x-y}Co_xM_yO_2$ (M=Al, Mn) cathode materials for lithium ion batteries, J. Power Sources 166 (2007) 233–238.
[13] H.S. Liu, Z.R. Zhang, Z.L. Gong, Y. Yang, Origin of deterioration for $LiNiO_2$ cathode

material during storage in air, Electrochem. Solid-State Lett. 7 (2004) A190–A193.

[14] S.W. Woo, S.T. Myung, H. Bang, D.W. Kim, Y.K. Sun, Improvement of electro-chemical and thermal properties of LiNi$_{0.8}$Co$_{0.1}$Mn$_{0.1}$O$_2$ positive electrode materials by multiple metal (Al, Mg) substitution, Electrochim. Acta 54 (2009) 3851–3856.

[15] F. Wu, M. Wang, Y.F. Su, L.Y. Bao, S. Chen, A novel layered material of LiNi$_{0.32}$Mn$_{0.33}$Co$_{0.33}$Al$_{0.01}$O$_2$ for advanced lithium-ion batteries, J. Power Sources 195 (2010) 2900–2904.

[16] J. Eom, K.S. Ryu, J. Cho, Dependence of electrochemical behavior on concentration and annealing temperature of Li$_x$CoPO$_4$ phase-grown LiNi$_{0.8}$Co$_{0.16}$Al$_{0.04}$O$_2$ cathode materials, J. Electrochem. Soc. 155 (2008) A228–A233.

[17] S.U. Woo, C.H. Kim, S.B. Kim, K. Amine, Y.K. Sun, Improvement of electrochemical performance of AlF$_3$-coated LiNi$_{0.8}$Co$_{0.1}$Mn$_{0.1}$O$_2$, Electrochem. Soc. 154 (2007) A1005–A1009.

[18] A.T. Appapillai, A.N. Mansour, J.P. Cho, S.H. Yang, Microstructure of LiCoO$_2$ with and without "AlPO$_4$" nanoparticle coating: combined STEM and XPS studies, Chem. Mater. 19 (2007) 5748–5757.

[19] X.H. Yu, J.B. Bates, G.E. Jellison, F.X. Hart, A stable thin-film lithium electrolyte: lithium phosphorus oxynitride (Lipon), J. Electrochem. Soc. 144 (1997) 524–532.

[20] Y.H. Cho, Y.S. Lee, S.A. Park, Y. Lee, J. Cho, LiNi$_{0.8}$Co$_{0.15}$Al$_{0.05}$O$_2$ cathode materials prepared by TiO$_2$ nanoparticle coatings on Ni$_{0.8}$Co$_{0.15}$Al$_{0.05}$(OH)$_2$ precursors, Electrochim. Acta 56 (2010) 333–339.

[21] J. Wang, B. Qiu, H. Cao, Y. Xia, Z. Liu, Electrochemical properties of 0.6Li[Li$_{1/3}$Mn$_{2/3}$]O$_2$-0.4LiNi$_x$Mn$_y$Co$_{1-x-y}$O$_2$ cathode materials for lithium-ion batteries, J. Power Sources 218 (2012) 128–133.

[22] X. Bian, Q. Fu, X. Bie, P. Yang, H. Qiu, Q. Pang, G. Chen, F. Du, Y. Wei, Improved electrochemical performance and thermal stability of Li-excess Li$_{1.18}$Co$_{0.15}$Ni$_{0.15}$Mn$_{0.52}$O$_2$ cathode material by Li$_3$PO$_4$ surface coating, Electrochim. Acta 174 (2015) 875–884.

[23] K.J. Kim, Y.N. Jo, W.J. Lee, T. Subburaj, K. Prasanna, C.W. Lee, Effects of inorganic salts on the morphological, structural, and electrochemical properties of prepared nickel-rich Li[Ni$_{0.6}$Co$_{0.2}$Mn$_{0.2}$]O$_2$, J. Power Sources 268 (2014) 349–355.

[24] H.Z. Zhang, Q.Q. Qiao, G.R. Li, S.H. Ye, X.P. Gao, Surface nitridation of Li-rich layered Li(Li$_{0.17}$Ni$_{0.25}$Mn$_{0.58}$)O$_2$ oxide as cathode material for lithium battery, J. Mater. Chem. 22 (2012) 13104–13109.

[25] C. Fu, G. Li, D. Luo, Q. Li, J. Fan, L. Li, Nickel-rich layered microspheres cathodes: lithium/nickel disordering and electrochemical performance, ACS Appl. Mater. Interfaces 6 (2014) 15822–15831.

[26] P. Mohan, G.P. Kalaignan, Electrochemical performances of co-substituted (La and Li) LiLa$_{x-y}$Li$_y$Ni$_{1-x}$O$_2$ cathode materials for rechargeable lithium-ion batteries, Mater. Res. Bull. 48 (2013) 3049–3057.

[27] M. Sumita, Y. Tanaka, M. Ikeda, T. Ohno, Theoretically designed Li$_3$PO$_4$ (100)/ LiFePO$_4$ (010) coherent electrolyte/cathode interface for all solid-state Li ion secondary batteries, J. Phys. Chem. C 119 (2015) 14–22.

[28] N. Wu, Y. Zhang, Y. Guo, S. Liu, H. Liu, H. Wu, Flakelike LiCoO$_2$ with exposed {010} facets as a stable cathode material for highly reversible lithium storage, ACS Appl. Mater. Interfaces 8 (2016) 2723–2731.

[29] L. Li, L. Wang, X. Zhang, M. Xie, F. Wu, R. Chen, Structural and electrochemical study of hierarchical LiNi$_{1/3}$Co$_{1/3}$Mn$_{1/3}$O$_2$ cathode material for lithium-ion batteries, Appl. Mater. Interfaces 7 (2015) 21939–21947.

[30] K. Kang, Y.S. Meng, J. Bréger, C.P. Grey, G. Ceder, Electrodes with high power and high capacity for rechargeable lithium batteries, Science 311 (2006) 977–980.

[31] J. Yang, M. Hou, S. Haller, Y. Wang, C. Wang, Y. Xia, Improving the cycling performance of the layerd Ni-rich oxide cathode by introduing low-content Li$_2$MnO$_3$, Electrochim. Acta 189 (2016) 101–110.

[32] K.S. Ryu, S.H. Lee, B.K. Koo, J.W. Lee, K.M. Kim, Y.J. Park, Effects of Co$_3$(PO$_4$)$_2$ coatings on LiNi$_{0.8}$Co$_{0.16}$Al$_{0.04}$O$_2$ cathodes during application of high current, J. Appl. Electrochem. 38 (2008) 1385–1390.

[33] F. Wu, M. Wang, Y.F. Su, S. Chen, B. Xu, Effect of TiO$_2$-coating on the electrochemical performances of LiCo$_{1/3}$Ni$_{1/3}$Mn$_{1/3}$O$_2$, J. Power Sources 191 (2009) 628–632.

[34] J. Wang, C. Du, C. Yan, X. He, B. Song, Al$_2$O$_3$ coated concentration-gradient Li [Ni$_{0.73}$Co$_{0.12}$Mn$_{0.15}$]O$_2$ cathode material by freeze drying for long-life lithium ion batteries, Electrochim. Acta 174 (2015) 1185–1191.

[35] J.H. Wang, Y. Wang, Y.Z. Guo, Z.Y. Ren, C.W. Liu, Effect of heat-treatment on the surface structure and electrochemical behavior of AlPO$_4$-coated LiNi$_{1/3}$Co$_{1/3}$Mn$_{1/3}$O$_2$ cathode materials, J. Mater. Chem. A 1 (2013) 4879–4884.

[36] C.H. Heum, D.H. Cho, H.J. Noh, H. Yashiro, Y.K. Sun, An effective method to reduce residual lithium compounds on Ni-rich Li[Ni$_{0.6}$Co$_{0.2}$Mn$_{0.2}$]O$_2$ active material using a phosphoric acid derived Li$_3$PO$_4$ nanolayer, Nano Res. 8 (2015) 1464–1479.

[37] Y.K. Na, T. Yim, J.H. Song, J.S. Yu, Z.H. Lee, Microstructural study on degradation mechanism of layered LiNi$_{0.6}$Co$_{0.2}$Mn$_{0.2}$O$_2$ cathode materials by analytical transmission electron microscopy, J. Power Sources 307 (2016) 641–648.

[38] F. Lin, I.M. Markus, D. Nordlund, T.C. Weng, M.D. Asta, H.L. Xin, M.M. Doeff, Surface reconstruction and chemical evolution of stoichiometric layered cathode materials for lithium-ion batteries, Nat. Commun. 5 (2014) 3529–3537.

[39] S.K. Jung, H. Gwon, J. Hong, K.Y. Park, D.H. Seo, H. Kim, J. Hyun, W. Yang, K. Kang, Understanding the degradation mechanisms of LiNi$_{0.5}$Co$_{0.2}$Mn$_{0.3}$O$_2$ cathode material in lithium ion batteries, Adv. Energy Mater. 4 (2014) 94–98.

[40] S. Hwang, W.Y. Chang, S.M. Kim, D. Su, D.H. Kim, J.Y. Lee, K.Y. Chung, E.A. Stach, Investigation of changes in the surface structure of Li$_x$Ni$_{0.8}$Co$_{0.15}$Al$_{0.05}$O$_2$ cathode materials induced by the initial charge, Chem. Mater. 26 (2014) 1084–−1092.

[41] S. Watanabe, M. Kinoshita, T. Hosokawa, K. Morigaki, K. Nakura, Capacity fade of LiAl$_y$Ni$_{1-x-y}$Co$_x$O$_2$ cathode for lithium-ion batteries during accelerated calendar and cycle life tests (surface analysis of LiAl$_y$Ni$_{1-x-y}$Co$_x$O$_2$ cathode after cycle tests in restricted depth of discharge ranges), J. Power Sources 58 (2014) 210–217.

[42] D.J. Miller, C. Proff, J.G. Wen, D.P. Abraham, J. Bareño, Observation of microstructural evolution in Li battery cathode oxide particles by in situ electron microscopy, Adv. Energy Mater. 3 (2013) 1098–1103.

[43] J. Yang, M. Hou, S. Haller, Y.G. Wang, C.X. Wang, Y.Y. Xia, Improving the cycling performance of the layered Ni-rich oxide cathode by introducing low-content Li$_2$MnO$_3$, Electrochim. Acta 189 (2015) 101–110.

[44] Y.K. Sun, J.M. Han, S.T. Myung, S.W. Lee, K. Amine, Significant improvement of high voltage cycling behavior AlF$_3$-coated LiCoO$_2$ cathode, Electrochem. Commun. 8 (2006) 821–826.

[45] Q. Cao, H.P. Zhang, G.J. Wang, Q. Xia, Y.P. Wu, H.Q. Wu, A novel carbon-coated LiCoO$_2$ as cathode material for lithium ion battery, Electrochem. Commun. 9 (2007) 1228–1232.

[46] Y.Q. Qiao, J.P. Tu, X.L. Wang, J. Zhang, Y.X. Yu, C.D. Gu, Self-assembled synthesis of hierarchical waferlike porous Li-V-O composites as cathode materials for lithium ion batteries, J. Phys. Chem. C 115 (2011) 25508–25518.